

## Torsional Control of Epoxidation Stereoselectivity in 1,2-Dihydronaphthalenes. Transition State Modeling with Semiempirical Quantum Mechanics

Melissa J. Lucero and K. N. Houk\*

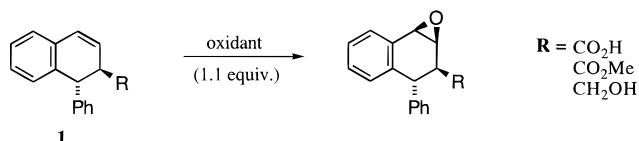
Department of Chemistry and Biochemistry, University of California, Los Angeles, California 90095-1569

Received April 22, 1998

Recently, highly diastereoselective epoxidations of chiral 1,2-dihydronaphthalenes were reported. Crystallographic characterization of the major product indicated that the selectivity cannot be attributed to long-range steric effects. We examined this system through *ab initio* and semiempirical quantum mechanical modeling. Corroborating experimental data, our investigations explain the apparent irrelevance of direct interactions with substituents and address the insensitivity of the stereoselectivity to oxidant structure. Furthermore, extension of this model to other related epoxidation reactions indicates that  $\pi$ -facial discrimination may be interpreted as a result of a preference for a staggered asynchronous transition state, obtainable only through axial attack.

### Introduction

The startling example of high stereoselectivity observed for the epoxidation of **1**, depicted in Figure 1, has recently been attributed to long-range steric effects.<sup>1</sup> Interestingly, such high selectivity was maintained despite variation of the substituent, R, or modification of the oxidant: both *m*-chloroperbenzoic acid (*m*-CPBA) and dimethyldioxirane (DMD) react with diastereomeric excesses (d.e.) over 95%.



In these systems, studied by Linker and co-workers, the oxidant attacks on the face anti to that of the phenyl group. A hydroxy directing effect<sup>2</sup> may be ruled out as the source of such preferential  $\pi$ -facial attack due to the fact that an acid, a homoallylic alcohol, and an ester all produce the same d.e. Although a steric effect involving phenyl group interaction with the oxidant was cited, an X-ray structure<sup>3</sup> of the preferred product, obtained for the system where R = CO<sub>2</sub>Me, indicates that there is no significant difference between the two faces of such a 1,2-dihydronaphthalene (Figure 1). The structure exhibits the expected diequatorial conformation,<sup>4</sup> indicating that the phenyl group is too far away to block either  $\pi$ -face of the precursor cyclohexene ring. The R groups are not likely to assist the approaching oxidant in any way. Thus, neither the allylic substituents, R, nor the phenyl group can be expected to exert significant stereocontrol.

(1) Linker, T.; Peters, K.; Peters, E.-M.; Rebien, F. *Angew. Chem., Int. Ed. Engl.* **1996**, *35*, 2487.

(2) Hoveyda, A. H.; Evans, D. A.; Fu, G. C. *Chem. Rev.* **1993**, *93*, 1307.

(3) Detailed structural data may be obtained from Fachinformationszentrum Karlsruhe, D-76344 Eggenstein-Leopoldshafen, Germany (Depository number CSD-405437).

(4) Rabideau, P. W.; Sygula, A. *The Conformational Analysis of Cyclohexenes, Cyclohexadienes, and Related Heteroaromatic Compounds*; VCH: Weinheim, 1989; pp 77–81.

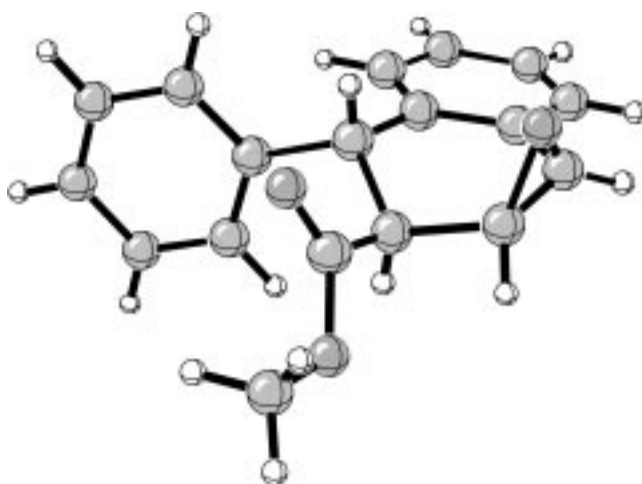


**Figure 1.** X-ray structure for the predominant epoxidation product of **1**.

Experimental precedent and recent work in our group provided a clue as to the source of this selectivity. Over forty years ago, Corey and Snee postulated that electrophilic attack on cyclohexenes occurs from an axial direction.<sup>5</sup> Furthermore, Toromanoff has analyzed torsional angle changes that occur for a variety of related reactions,<sup>6</sup> Vedejs *et al.*<sup>7</sup> have investigated the significance of torsional effects and preference for axial attack in the epoxidations of 4-*tert*-butylmethylenecyclohexane, and Ducrot and co-workers<sup>8</sup> showed the same preference for axial attack exists in the stereoselective alkene epoxidations observed for flexible polycyclic systems. We have demonstrated how preferences such as this may be understood in terms of torsional effects in the transition

(5) Corey, E. J.; Snee, R. A. *J. Am. Chem. Soc.* **1956**, *78*, 6269.

(6) Toromanoff, E. *Tetrahedron* **1980**, *78*, 6269.

(7) Vedejs, E.; Dent, W. H., III; Kendall, J. T.; Oliver, P. A. *J. Am. Chem. Soc.* **1996**, *118*, 3556.

(8) Ducrot, P.; Bucourt, R.; Thal, C.; Marçot, B.; Mayrargue, J.; Moskowicz, H. *Tetrahedron* **1996**, *52*, 6699.

state.<sup>9</sup> Torsional effects "steer" the electrophile so that it attacks in a manner conducive to minimization of eclipsing interactions between the forming bond and the allylic C–H bond. Consequently, we have undertaken a theoretical study to determine whether these torsional effects, or the steric effects proposed by Linker et al., cause the remarkable stereoselectivity of this reaction.

### Computational Methods

Semiempirical geometry optimizations for all systems were carried out at the PM3 level of theory implemented in SPARTAN.<sup>10</sup> Each transition structure gave only one imaginary harmonic vibrational frequency corresponding to the formation of new C–O bonds. The activation energies were estimated from RHF/6-31G\* single-point calculations on the PM3-optimized geometries using Gaussian 94.<sup>11</sup>

### Results and Discussion

While quantum mechanical methods such as B3LYP are now available to provide accurate transition states for such reactions, a study of systems the size of 1,2-dihydronaphthalenes (1,2-DHNs) is still prohibitively time-consuming. In the past, we developed force field transition state models for such cases and applied them successfully.<sup>12</sup> While we obtained promising results for epoxidations using this method, we chose to investigate the use of semiempirical quantum mechanics and compare these results to our B3LYP studies,<sup>13</sup> which demonstrated that the peracid oxidation of alkenes proceeds through a *spiro* transition state. For substituted alkenes, such as butadiene, bond formation is *asynchronous*, whereas in the case of ethylene, the transition state is symmetrical. In our semiempirical PM3 studies, the transition states for the reactions of ethylene and butadiene with performic acid were located (Figure 2) and found to parallel the B3LYP geometries, showing a spiro and synchronous transition state for ethylene and a spiro, asynchronous transition state for butadiene. They differ in that PM3 gives a much later transition state in terms of the C–O distances, and the PM3-derived butadiene transition state is less asynchronous.

Having established the reliability of semiempirical methods, the transition structures for the performic acid epoxidation of the 1,2-DHN, where R = CO<sub>2</sub>H, were located using PM3 and are illustrated in Figure 3. Attack from either face resulted in a spiro orientation of the peracid and asynchronous C–O bond formation, as

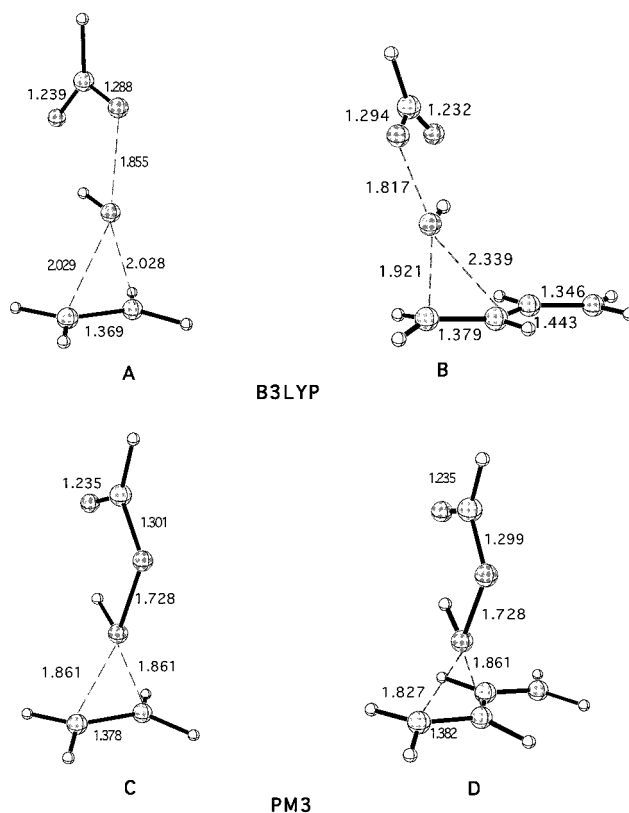


**Figure 2.** Comparison of B3LYP and PM3 transition structures for the epoxidations of ethylene and butadiene by performic acid.

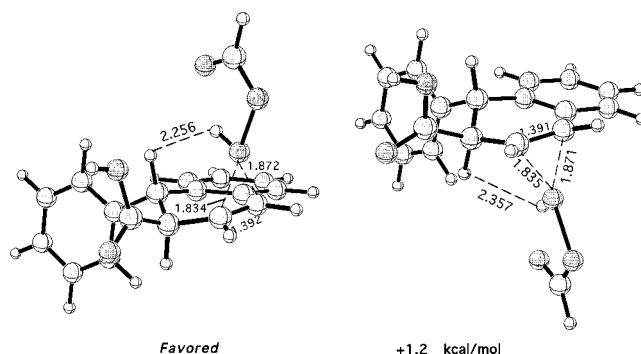


**Figure 3.** Transition structures for the performic acid epoxidation of **1**, where R = CO<sub>2</sub>H.

in the model reactions. In both cases, the shortest C–O bond length involves C2, the sp<sup>2</sup> carbon furthest from the aromatic ring, with a 1.834 Å distance for approach from the top face and a 1.835 Å for attack syn to the phenyl. The longer bond lengths are 1.872 and 1.871 Å, respectively.

The RHF/6-31G\* single-point energies calculated for the PM3 geometries correctly identify the favored product, corresponding to epoxidation occurring on the face anti to that of the phenyl. The transition state for anti attack is 1.2 kcal/mol more stable than attack from the opposite face. Closer examination of the favored transition structure indicates that the shorter of the forming C–O bonds is in a staggered orientation relative to the substituents on C3, whereas the disfavored transition structure shows significant eclipsing between the forming bond and the allylic hydrogen of C3. As the Newman projections in Figure 4 indicate, the favored, staggered

(9) (a) Rondan, N. G.; Paddon-Row, M. N.; Caramella, P.; Mareda, J.; Mueller, P. H.; Houk, K. N. *J. Am. Chem. Soc.* **1982**, *104*, 4974. (b) Paddon-Row, M. N.; Rondan, N. G.; Houk, K. N. *J. Am. Chem. Soc.* **1982**, *104*, 7162. (c) Houk, K. N.; Paddon-Row, M. N.; Rondan, N. G.; Wu, Y.-D.; Brown, F. K.; Spellmeyer, D. C.; Metz, J. T.; Li, Y.; Loncharich, R. J. *Science* **1986**, *231*, 1108. (d) Martinelli, M. J.; Peterson, B. C.; Khau, V. V.; Hutchison, D. R.; Leanna, M. R.; Audia, J. E.; Droste, J. J.; Wu, Y.-D.; Houk, K. N. *J. Org. Chem.* **1994**, *59*, 2204.

(10) SPARTAN version 4.0; Wavefunction, Inc., 18401 Von Karman Ave., #370, Irvine, CA 92715, 1995.

(11) Gaussian 94, Revision D.3: Frisch, M. J.; Trucks, G. W.; Schlegel, H. B.; Gill, P. M. W.; Johnson, B. G.; Robb, M. A.; Cheeseman, J. R.; Keith, T.; Petersson, G. A.; Montgomery, J. A.; Raghavachari, K.; Al-Laham, M. A.; Zakrzewski, V. G.; Ortiz, J. V.; Foresman, J. B.; Cioslowski, J.; Stefanov, B. B.; Nanayakkara, A.; Challacombe, M.; Peng, C. Y.; Ayala, P. Y.; Chen, W.; Wong, M. W.; Andres, J. L.; Replogle, E. S.; Gomperts, R.; Martin, R. L.; Fox, D. J.; Binkley, J. S.; Defrees, D. J.; Baker, J.; Stewart, J. P.; Head-Gordon, M.; Gonzalez, C.; Pople, J. A. Gaussian, Inc., Pittsburgh, PA, 1995.

(12) Eksterowicz, J. E.; Houk, K. N. *Chem. Rev.* **1993**, *93*, 2439.

(13) Houk, K. N.; Liu, J.; DeMello, N. C.; Condroski, K. R. *J. Am. Chem. Soc.* **1997**, *119*, 10147.

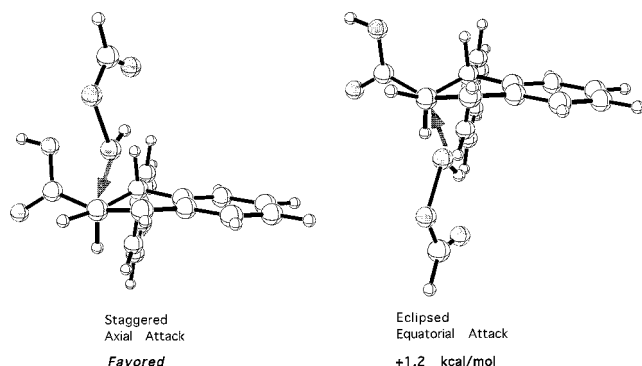


**Figure 4.** Staggered and eclipsed orientations of the forming bond as the result of axial and equatorial attack on **1a**.

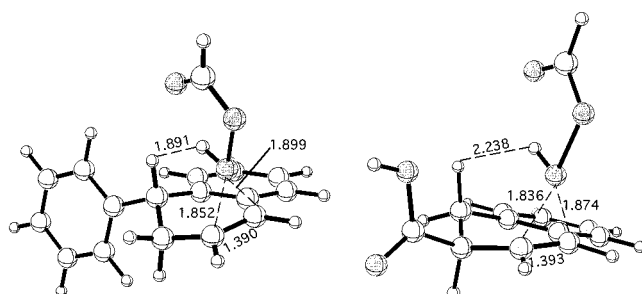
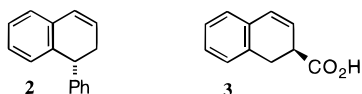


**Figure 5.** Favored transition structures for performic acid epoxidation of **2** and **3**.

arrangement in the more stable transition structure results from an axial attack of the peracid, whereas equatorial attack results in significant eclipsing interactions.

To confirm the absence of any significant steric effects and to investigate the magnitude of torsional effects, we investigated the 1,2-DHNs related to the Linker molecule, where the allylic substituent, **2**, and phenyl group, **3**, have been removed. Interestingly, in both instances, attack from the axial position is favored, corresponding to product formation anti to the phenyl and syn to the substituent on C3. The favored transition structures for both systems are illustrated in Figure 5.



In the favored transition structure for the epoxidation of **2**, the asynchronicity of the transition state is more pronounced than in the Linker system, with a short C–O bond distance of 1.852 Å and a long C–O distance of 1.899 Å. For **3**, the forming bond distances are 1.836 and 1.874 Å, respectively. Just as in **1**, the transition states for these systems may be characterized by a preference for a staggered arrangement of the forming C–O bond, resulting from an axial approach of the oxidant. The data for all 1,2-DHNs modeled are summarized in Table 1. We thus propose that the stereoselectivity discovered by Linker *et al.* arises from the interplay of torsional effects in the proximity of the forming bond and *not* from hindrance of a  $\pi$ -face or as the result of “steering” by a heteroatom.

The apparent insensitivity of **1** to the nature of the oxidant is similarly explained by a torsional steering model. Torsional effects in the proximity of the C–O

**Table 1.** Modeling of the Epoxidations of **1–3**

Compound	Approach*	Peracid H Orientation	Energy (kcal/mol) <sup>†</sup>		Mode of Attack
			PM3	RHF/6-31G*	
<b>1</b>	Anti	in	0.0	0.0	axial
	Syn	in	0.2	1.2	equatorial
<b>2</b>	Anti	in	0.0	0.0	axial
	Syn	in	0.2	1.0	equatorial
<b>3</b>	Anti	in	0.0	0.0	axial
	Syn	out	0.4	4.6	equatorial

\* Relative to the phenyl group.

<sup>†</sup> RHF/6-31G\* single point calculations on the PM3 optimized geometries.

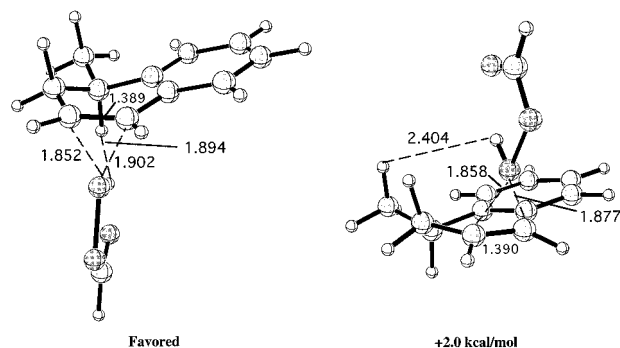
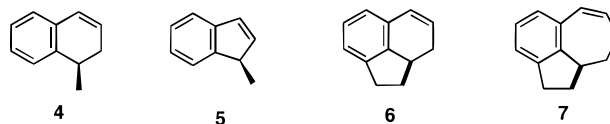


**Figure 6.** PM3 transition structures for performic acid epoxidation of **4**.

bond forming at C2 are what control the stereoselectivity, so the most relevant atoms in each oxidant molecule would be those involved in the formation of the C–O bonds, i.e., the steric bulk and torsional effects in the region of the transferred oxygen are what matters, not the groups attached to the oxygen. The relevant bulk of performic acid, *m*-CPBA, and DMD is, therefore, almost identical.

We also tested the PM3 model on related systems studied earlier.<sup>9d</sup> We examined the extent of applicability for this model by studying the variety of substitution patterns exhibited by the carbon analogues of the so-called partial ergot alkaloids and related compounds.



The experimentally observed stereoselectivity calculated for **4** indicates an 85:15 preference for attack anti to the methyl group. Our model correctly predicts the favored product, with attack syn to the methyl group disfavored by 2.0 kcal/mol. The transition structures are illustrated in Figure 6. The favored transition state, corresponding to an axial attack of performic acid, is asynchronous, with C–O bond lengths of 1.852 and 1.894 Å. The shorter of the forming C–O bonds is staggered nicely relative to the equatorially oriented allylic hydrogen. The disfavored product, on the other hand, is less asynchronous, with forming C–O bond lengths of 1.858 and 1.877 Å and the shorter C–O bond is eclipsing the axially oriented allylic proton. This case is interesting because the selectivity again favors attack from the face opposite that of the substituent in the 4-position, which is remarkable considering that the methyl group is much smaller than the phenyl group. Additionally, the pre-

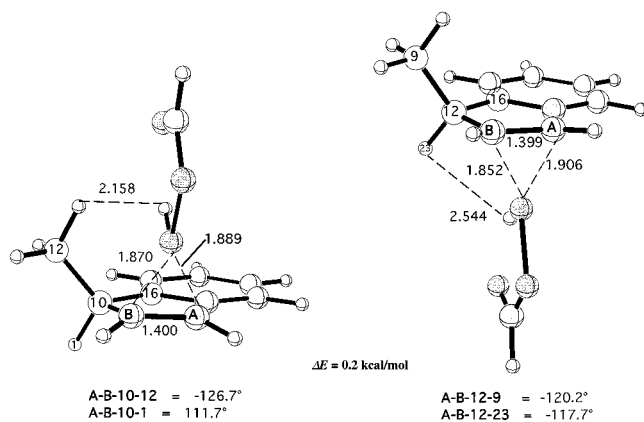


**Figure 7.** PM3 transition structures for performic acid epoxidation of **5**.

ferred epoxide forms on the bottom face, whereas in the case of the Linker 1,2-DHN the preferred epoxide formed on the top face. Closer examination shows that the half-chair conformations of **1** and **4** are different. Nevertheless, what is important to selectivity is neither the size of the substituent at C4 nor the ring conformation. Torsional steering, the preference for a staggered arrangement of the forming C–O bond, is the source of stereocontrol in this reaction.

Our model also reproduces the experimentally observed lack of selectivity observed in the oxidation of methylindene, **5**. The transition structures, illustrated in Figure 7, are again asynchronous, but not to the same extent observed in **4**. The forming C–O bond lengths in the syn attack are 1.870 and 1.889 Å, whereas those for anti attack are 1.852 and 1.906 Å. Due to the presence of the planar C5 ring, the torsional strain imparted by approaching anti to the methyl group is effectively the same as the approach anti to the hydrogen, and thus, no selectivity is observed. Our model predicts only a 0.2 kcal/mol energy difference between the two approaches, “favoring” attack anti to the methyl group. The lack of selectivity arises from the inability to arrive at a more staggered transition state because the C–Me and C–H angles relative to the plane of the ring are nearly identical (Figure 7). Neither the methyl nor the hydrogen is either axial or equatorial; therefore facial discrimination on the basis of torsional effects is nonexistent. The lack of selectivity in the absence of torsional steering underscores the importance of torsional effects and demonstrates the insignificance of steric effects imparted by substituents, even when they are allylic.

The preferred transition structures for compound **6** are illustrated in Figure 8. Experimentally, a 99:1 d.e. was observed, favoring the epoxide formed syn to the C4 proton. Axial attack, resulting in a staggered orientation for bond formation, is again favored; therefore the predominant epoxide is that which forms on the bottom, en face. This preference is remarkable in that the underside of the molecule could be thought of as more congested due to the presence of the C4 proton. Nevertheless, torsional effects override this potential steric impediment and the performic acid attacks from the bottom face with its proton facing in toward the C4 proton, despite the 1.95 Å distance between them.

The facial selectivity in the reactions of **7** is the reverse of that observed for the other systems; experimentally, the favored product is that which results from addition

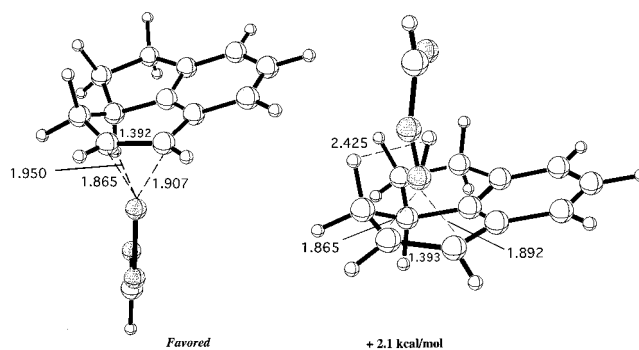


**Figure 8.** PM3 transition structures for performic acid epoxidation of **6**.

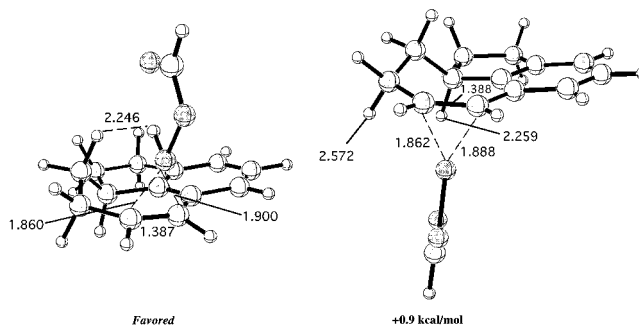


**Figure 9.** PM3 transition structures for performic acid epoxidation of **7**.

**Table 2.** PM3 Investigation of Epoxidation of Compounds 4–7

Compound	Epoxide	Exptl Ratio	Peracid H Orientation	PM3 Energy (kcal/mol) <sup>†</sup>	RHF/6-31G* Energy (kcal/mol) <sup>‡</sup>	Mode of Attack
<b>4</b>	en	85	in	0.0	0.0	axial
	zu	15	in	1.2	2.0	equatorial
<b>5</b>	zu	50	in	0.0	0.0	axial
	en	50	in	0.1	0.2	equatorial
<b>6</b>	en	99	in	0.0	0.0	axial
	zu	1	in	1.5	2.1	equatorial
<b>7</b>	en	18	in	0.4	0.9	equatorial
	zu	82	in	0.0	0.0	axial

syn to the substituent, or attack from the zu face.<sup>9d</sup> The reversal of selectivity may be explained in terms of the conformation of the seven-membered ring. The most stable conformation for the cycloheptene has the carbon  $\alpha$  to the ring fusion oriented out of the plane, in the direction of the zu face (Figure 9). Staggered attack at C2 corresponds to an approach from the zu face. In this case, the steric congestion encountered on the en face might be implicated as the source, but as was demonstrated in the study of **6**, torsional strain predominates. Furthermore, if the peracid proton–homoallylic proton interaction were a significant contributor, the facial selectivity would actually parallel the facial selectivity observed in **6**, since the en face would then be favored. Moreover, if this were truly the case, then the selectivity should be higher in **7** than in **6**, where no such interaction exists. In fact, the experimental data indicates that the selectivity for **6** is much higher than in **7**, 99:1 as compared to 82:18, and the facial selectivity is *opposite* to that of the previously studied systems. The selectivity is best explained as the result of torsional steering in the

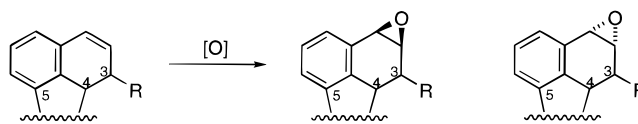
transition state. The data for this and all of the other highly substituted systems are summarized in Table 2.

### Conclusion

It is clear that our model correlates well with experiment, successfully identifying the favored product for all molecules studied. Furthermore, each of the favored transition structures has the oxidant attacking in an axial fashion, leading to a staggered arrangement of the forming bond. This behavior strongly suggests that torsional control is operative. We have thus demonstrated that this pattern of axial attack is pervasive throughout an entire series of 1,2-dihydronaphthalenes (Scheme 1).

The presence of R groups  $\alpha$  and  $\beta$  to the forming bond impart an effect only in that they help fix the half-chair conformation of the transition state, which in turn dictates which  $\pi$ -face will result in axial attack. Our semiempirical model thus strongly indicates that oxidant

### Scheme 1



$\pi$ -facial discrimination is the consequence of a large preference for a torsionally unencumbered transition state, obtainable only through staggering of the forming bond, resulting from axial attack.

**Acknowledgment.** We are grateful to the National Institute of General Medical Sciences, National Institutes of Health for financial support of this research, the Dorothy Danforth-Compton Foundation for a fellowship to M.J.L., and to Dr. Thomas Strassner for his contribution to the conversion and graphical representation of the X-ray data.

JO980760G